Late Miocene Onset of Tasman Leakage and Southern Hemisphere Supergyre Ushers in Near-Modern Circulation

Beth A. Christensen[1] ![ORCID], David De Vleeschouwer[2] ![ORCID], Jorijntje Henderiks[3] ![ORCID], Jeroen Groeneveld[4,5] ![ORCID], Gerald Auer[6] ![ORCID], Anna Joy Drury[7], Boris Theofanis Karatsolis[3] ![ORCID], Jing Lyu[2], Christian Betzler[5], Gregor P. Eberli[8], and Dick Kroon[9]

[1]Department of Environmental Science, School of Earth and Environment, Rowan University, Glassboro, NJ, USA, [2]MARUM–Center for Marine Environmental Sciences, University of Bremen, Bremen, Germany, [3]Department of Earth Sciences, Uppsala University, Uppsala, Sweden, [4]Department of Geosciences, Bremen University, Bremen, Germany, [5]Department of Earth Sciences, Hamburg University, Hamburg, Germany, [6]Institute of Earth Sciences (Geology and Paleontology), NAWI Graz Geocenter, University of Graz, Graz, Austria, [7]Department of Earth Sciences, University College London, London, UK, [8]Department of Geosciences, Rosenstiel School of Marine and Atmospheric Science, University of Miami, Miami, FL, USA, [9]School of Geosciences, University of Edinburgh, Edinburgh, UK

Abstract This study provides a Miocene-to-recent history of Tasman Leakage (TL), driving surface-to-intermediate waters from the Pacific into the Indian Ocean. TL, in addition to Indonesian ThroughFlow (ITF), constitutes an important part of the Southern Hemisphere Supergyre. Here, we employ deep-sea benthic δ^{13}C timeseries from the southwestern Pacific and eastern Indian Oceans to identify the history of Tasman Leakage. The δ^{13}C results combined with sedimentary evidence show that an inter-ocean connection south of Australia existed from 7 Ma onward. A southward shift in Westerlies combined with a northward movement of Australia created the oceanic corridor necessary for Tasman Leakage (between Australia and the sub-Antarctic Front) at this time. Furthermore, changes in the northern limb of the Supergyre (ITF) are evident in the sedimentary record on Broken Ridge from ~3 to 2 Ma when Banda Sea intermediate waters started originating from the North Pacific.

Plain Language Summary Global ocean circulation allows for the distribution of heat between different latitudes and different water depths. It has long been understood that much of the return flow from the Pacific to the Atlantic occurs through the Indonesian Throughflow, but more recently, oceanographers have identified another, deeper pathway south of Australia: the Tasman Leakage. This connection consists of Pacific waters that leave the Tasman Sea by flowing southwest around Australia, into the Indian Ocean and ultimately back into the Atlantic. We use carbon isotopes of benthic foraminifera, coupled with sedimentation patterns around Australia and the Indian Ocean, to determine the onset of this new pathway in global thermohaline circulation: This occurred around 7 Ma. This onset was coincident with major global climatic and oceanographic change and was controlled by the position of the Australian continent and the sub-Antarctic Front. TL onset was only able to occur when Australia had moved far enough north to allow for westward flow.

1. Introduction

The present-day interchange of water and heat between the Atlantic, Pacific, and Indian Oceans has been described through observation (physical properties and float studies) and numerical modeling at surface and intermediate water depths. The three ocean basin gyres of the Southern Hemisphere are strongly coupled in a system known as the Southern Hemisphere Supergyre (SHS). The Tasman Leakage (TL) branch of the SHS drives surface-to-intermediate waters from the Pacific into the Indian Ocean through an oceanic corridor/deeper pathway south of Australia (Figure 1). The SHS has become commonplace in discussions on past, present, and future thermohaline circulation, but the TL branch remains understudied and its geologic history largely unknown. In particular, the TL expression in the sedimentary record has not been established.
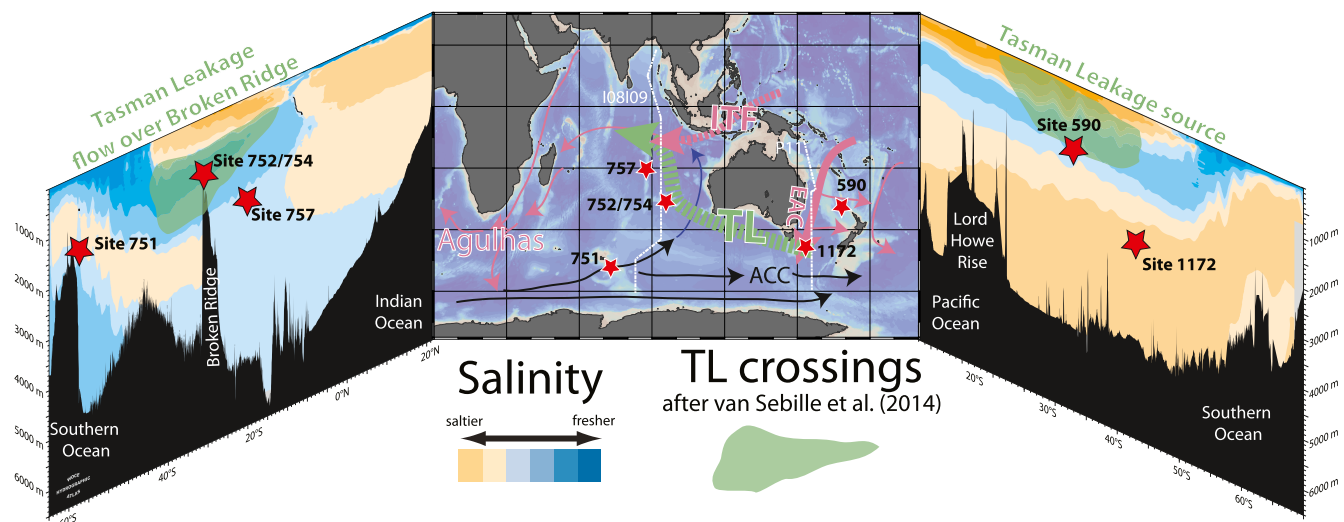
Figure 1. Inter-ocean connectivity between the Pacific and Indian Oceans through the Indonesian Throughflow (ITF) and Tasman Leakage (TL; after Lumpkin & Speer, 2007). TL crossings (green area; van Sebille et al., 2014) are superimposed on WOCE depth-latitude salinity sections (lines I08I09 and P11). These cross-sections illustrate Sites 590 and 752–754 as the TL end-member, while Sites 751 and 1172 constitute the Antarctic Intermediate Water (AAIW) end-member. (Note that Site 1172 paleodepth was shallower in the Miocene, e.g., Huck et al., 2017) TL intermediate waters are saltier (34.5–35.2 psu) than AAIW (~34.4 psu). East Australian Current (EAC) is the site of eddy formation. Note Banda Intermediate Water is not illustrated but flows from the ITF region westward with a limited southerly component of flow.

1.1. Modern Tasman Leakage and the Southern Hemisphere Supergyre

The SHS is an oceanographic concept introduced by Speich et al. (2007) and Ridgway and Dunn (2007), although earlier works describe ocean gyres linked through pathways north and south of Australia (Tilburg et al., 2001). From most to least intense, the contributing oceanic gyres linked in the SHS are the Indian, South Pacific, and Atlantic (Ridgway & Dunn, 2007). In the SHS concept, the Pacific and Indian surface waters function as one system via the Indonesian Throughflow (ITF), and the TL connects the South Pacific and Indian Oceans at intermediate depths (Ridgway & Dunn, 2007). ITF, TL, and Drake Passage waters converge in the Agulhas Current to complete the SHS (Durgadoo et al., 2017; Speich et al., 2002). Recent works hint at the significance of the SHS in the global ocean circulation and related impacts on regional climate patterns. For example, Duan et al. (2013) report a cooling and freshening of intermediate waters within the SHS over the last decades, in concert with a central-south Pacific-focused 2.5° southward shift in position. Behrens et al. (2019) detail the influence of enhanced TL on regional climate, including diminished meridional temperature gradients and westerlies in the Southern Ocean and resulting in a positive feedback (reduced AAIW formation and southward expansion of the SHS). Fan et al. (2020) suggested the SHS may control drought in South Australia, whereby TL constitutes the teleconnection between continental precipitation and the SHS. These new insights, coupled with the projection of enhanced TL flow in future decades (Oliver et al., 2015), highlight the need for a comprehensive understanding of the TL and its role in the SHS.

Present-day TL is focused at upper intermediate depths as determined from observations, models, and float studies (Ridgway & Dunn, 2007; Rintoul & Bullister, 1999; Speich et al., 2002, 2007; van Sebille et al., 2012, 2014; Figure 1). The East Australian Current (EAC) transports heat and high-salinity waters poleward to the mid-latitudes and into the Tasman Sea (Hu et al., 2015; Ridgway & Dunn, 2003; Sloyan & Rintoul, 2001; Figure 1). The TL originates when a portion of the EAC waters move westward around Tasmania within the upper 1,000 m of the water column (van Sebille et al., 2012, 2014) to form TL (Speich et al., 2007; Figure 1). When flowing between the Australian continent to the north and the Antarctic Circumpolar Current (ACC) to the south (Ridgway & Dunn, 2007), the TL core sits between 400 and 900 m water depth (van Sebille et al., 2014). Within this oceanic corridor, TL is influenced by the position of the Subtropical Front (STF; Rintoul & Sokolov, 2001) and Australia itself. Once past the Australian continent, TL flows in a northwesterly direction between 110 and 95°E (Speich et al., 2002) over the Broken Ridge (Figure 1). TL gradually blends in with the subtropical gyre (Durgadoo et al., 2017; Speich et al., 2002) flowing across the southern Indian Ocean from ~32°S to the Mascarene Plateau region (Ridgway & Dunn, 2007;

Speich et al., 2002), and partly directly feeding the Agulhas Current (Durgadoo et al., 2017). Retroflection from Southern Ocean AAIW and Agulhas Current somewhat freshen the high-salinity TL intermediate waters (Rintoul & Sokolov, 2001), but its salinity does not change much until reaching the Agulhas Current region (Ridgway & Dunn, 2007). Agulhas waters crossing the Cape of Good Hope are predominantly Pacific source water, with 50% of the water originating from the ITF and 42% from TL (Durgadoo et al., 2017).

The TL can be readily identified in salinity profiles around Australia (Figures 1 and S2; Table S1). TL flow is ~4 Sv in both modeling (van Sebille et al., 2012) and float (Rosell-Fieschi et al., 2013) studies, compared to 14.3 Sv through the ITF (van Sebille et al., 2014), whereas more recent modeling suggests a somewhat greater role for TL (Rousselet et al., 2020). TL flow varies seasonally (Rosell-Fieschi et al., 2013; van Sebille et al., 2012) and largely depends on large-scale wind patterns over the Pacific (van Sebille et al., 2014). Indeed, the surface waters that feed TL display the greatest seasonal variability, whereas the upper intermediate TL waters are more perennial (Rosell-Fieschi et al., 2013). At 115°E flow increases to 5.0 ± 1.8 Sv (Rosell-Fieschi et al., 2013), as the TL is strengthened with waters from an anticyclonic loop from 139 to 146°E located between the Great Australian Bight (GAB) and the ACC (Rintoul & Sokolov, 2001).

1.2. Tasman Leakage Importance in the Global Thermohaline Circulation

Global thermohaline circulation was long thought to be a relatively simple system: deep water formed in the North Atlantic was distributed globally via the ACC, with most return surface flow occurring from the North Pacific to the South Atlantic via the ITF and the Agulhas Current. The reality, however, is more complex (e.g., Talley, 2013), with the Indian Ocean increasingly seen as playing a more critical role in thermohaline circulation (Schott et al., 2009). It is now clear that both the ITF and TL are important inter-basinal connections that ultimately provide return waters for the North Atlantic through the Agulhas Current (Durgadoo et al., 2017; Rousselet et al., 2020). Flow through both the Tasman and Agulhas Leakages has been increasing over the past decades (Qu et al., 2019; Figure 1). Heat flux from the Pacific to the Indian through the TL is ~1/3 of the ITF flux (van Sebille et al., 2012), whereby TL may even compensate for decreasing ITF volumes during El Niño times (van Sebille et al., 2014). Modern studies are shedding light on regional impacts and feedbacks (Behrens et al., 2019; Duan et al., 2013; Fan et al., 2020) of the TL and its role in the SHS. Unraveling the mysteries of the TL in the past will help define the complexity of Indian Ocean circulation and its relationship to the Atlantic and Pacific Oceans and may illuminate the global controls displayed by the SHS.

1.3. Detecting Tasman Leakage in the Geologic Record

This paper seeks to advance the understanding of TL and the SHS by determining its onset as recorded in geologic archives. Thereby, our objective is to provide first-order answers to three open questions. (a) When did the TL originate? (b) Did TL impact ocean circulation and global climate? (c) Did ITF restriction influence Indian Ocean circulation at intermediate-water depths (AAIW, TL, and Banda Intermediate Water, BIW)? We explore regional circulation patterns from ~12 Ma onward, using benthic carbon-isotope and sedimentologic data from five sites (Figure 1). We employ $\delta^{13}C$ to identify TL and differentiate it from other water masses as previously demonstrated (e.g., Hodell & Venz-Curtis, 2006; Poore et al., 2006; Tian et al., 2018). We complement the $\delta^{13}C$ proxy with regional sedimentologic observations (hiatuses, winnowing, and slumping) to reconstruct past ocean circulation change. This combined approach allows pinpointing of TL onset in geologic time and suggests a combination of paleoceanographic and tectonic controls: TL onset was only able to occur when there was room for the current to flow west, south of Australia, and north of the sub-Antarctic Front.

2. Materials and Methods

This project draws on the legacy of scientific ocean drilling sediments and data. It utilizes previously published $\delta^{13}C_{benthic}$ records from sediments collected through scientific ocean coring (Deep Sea Drilling Project [DSDP]; Ocean Drilling Program [ODP]; International Ocean Discovery Program [IODP], Table 1). These lower resolution records of mostly single genera of benthic foraminifera are readily comparable, providing valuable insight into long-term, regional trends. Since high-resolution age-depth models are not applicable

Table 1
Sites and Locations Referenced in This Study

| Location	Expedition	Site/Hole	Water depth (m)	Latitude and longitude	Reference
Lord Howe Rise–Tasman Sea	DSDP Leg 90	590	1,299	31°10.02′S; 163°21.51′E	Kennett (1986)
Kerguelen Plateau	ODP Leg 120	751	1,633	57°43.56′S; 79°48.89′E	Mackensen et al. (1992)
Broken Ridge–Indian Ocean	ODP Leg 121	752	1,086	30°53.475′S; 93°34.652′E	Rea et al. (1991)
	ODP Leg 121	754	1,063	30°56.439′S; 93°33.991′E	House et al. (1992)
90E Ridge–Indian Ocean	ODP Leg 121	757	1,650	17°01.458′S; 88°10.899′E	Rea et al. (1991)
East Tasman Plateau	ODP Leg 189	1172A	2,620	43°57.5854′S; 149°55.6961′E	Diester-Haass et al. (2006)
Marion Plateau;W. Pacific	ODP Leg 194	---	–	–	Isern et al. (2002)
					Eberli et al. (2010)
Great Australian Bight	ODP Leg 182	---	–	–	Fearyet al. (2000)
Maldives	IODP Exp. 359	---	–	–	Betzler et al. (2016)

Note. DSDP, Deep Sea Drilling Project; IODP, International Ocean Discovery Program; ODP, Ocean Drilling Program.

for these sites, we created simple age-depth models by linear interpolation in-between calcareous nanno-plankton biostratigraphic datums (Table S2), updated to the GTS2012 (Gradstein et al., 2012). As a first-order assessment of the individual age-depth models, benthic foraminiferal $\delta^{18}O$ records of each study site were plotted against the $\delta^{18}O_{benthic}$ megasplice (De Vleeschouwer et al., 2017; Figure S5). Their congruency supports our linear age-depth conversion.

3. Results: Onset of the Tasman Outflow

Based on the modern system, we anticipate that the studied $\delta^{13}C_{benthic}$ records are largely dominated by two distinct signals: a South Pacific end-member (Tasman Sea/TL) and a Southern Ocean end-member (AAIW; Figure 1). Sites currently bearing a Pacific Ocean signature (DSDP Site 590 and ODP Sites 752 and 754) contrast with sites representing an AAIW signature (ODP Sites 751 and 1172; Figure 2). As expected, the AAIW sites largely track the Southern Ocean deep-water $\delta^{13}C$ signal (e.g., Poore et al., 2006) throughout the entire studied interval. The Broken Ridge Sites 752 and 754, on the other hand, only track the AAIW records until ~7 Ma, after which they diverge (Figure 2), suggesting the appearance of a more modern configuration. Prior to 7 Ma, Broken Ridge $\delta^{13}C$ values are ~0.3‰ heavier than AAIW sites $\delta^{13}C$, yet fall within the range for upper component deep waters reported by Hodell and Venz-Curtis (2006). DSDP Site 590 benthic $\delta^{13}C$ values exhibit strong similarity with Pacific deepwater $\delta^{13}C$ records of Cramer et al. (2009) prior to 7 Ma. At ~7 Ma, Site 590 $\delta^{13}C$ values rise to 1‰ as Pacific deepwater $\delta^{13}C$ falls below zero, indicating the influence of upper EAC rather than deep waters at DSDP Site 590 at intermediate depths. Therewith, DSDP Site 590 converges toward the Broken Ridge $\delta^{13}C$ values after 7 Ma. After ~7 Ma, the Broken Ridge and Site 590 $\delta^{13}C$ values are stable around 1‰ until Broken Ridge Sites 752 and 754 become more positive by ~0.5‰–1‰ between ~2.4 and 1.8 Ma (Figure 2) relative to DSDP Site 590.

The simultaneous convergence of TL benthic $\delta^{13}C$ and divergence between the Broken Ridge and AAIW $\delta^{13}C$ records support a ~7 Ma onset of waters flowing from the Tasman Sea into the Indian Ocean, supplying intermediate-depth bottom waters to Broken Ridge Sites 752 and 754. TL onset is thus synchronous with a late Miocene carbon isotope shift (LMCIS) in $\delta^{13}C$ in intermediate and deeper (Hodell & Venz-Curtis, 2006; Poore et al., 2006; Tian et al., 2018) waters, but the LMCIS alone does not explain our results. Before 7 Ma, all three locations closely follow global patterns in deepwater $\delta^{13}C$, reflecting the contributions of those water masses (Figure 2). However, at 7 Ma, only AAIW continues to follow the same patterns as the other oceanic records (e.g., Hodell & Venz-Curtis, 2006) as TL upper intermediate water comes into existence and determines the $\delta^{13}C$ signatures of Sites 590, 752, and 754. The ~7 Ma onset of the southern limb of the SHS corresponds with the change to more modern $\delta^{13}C$ gradients, particularly evident in South Atlantic and Pacific records (Hodell & Venz-Curtis, 2006).
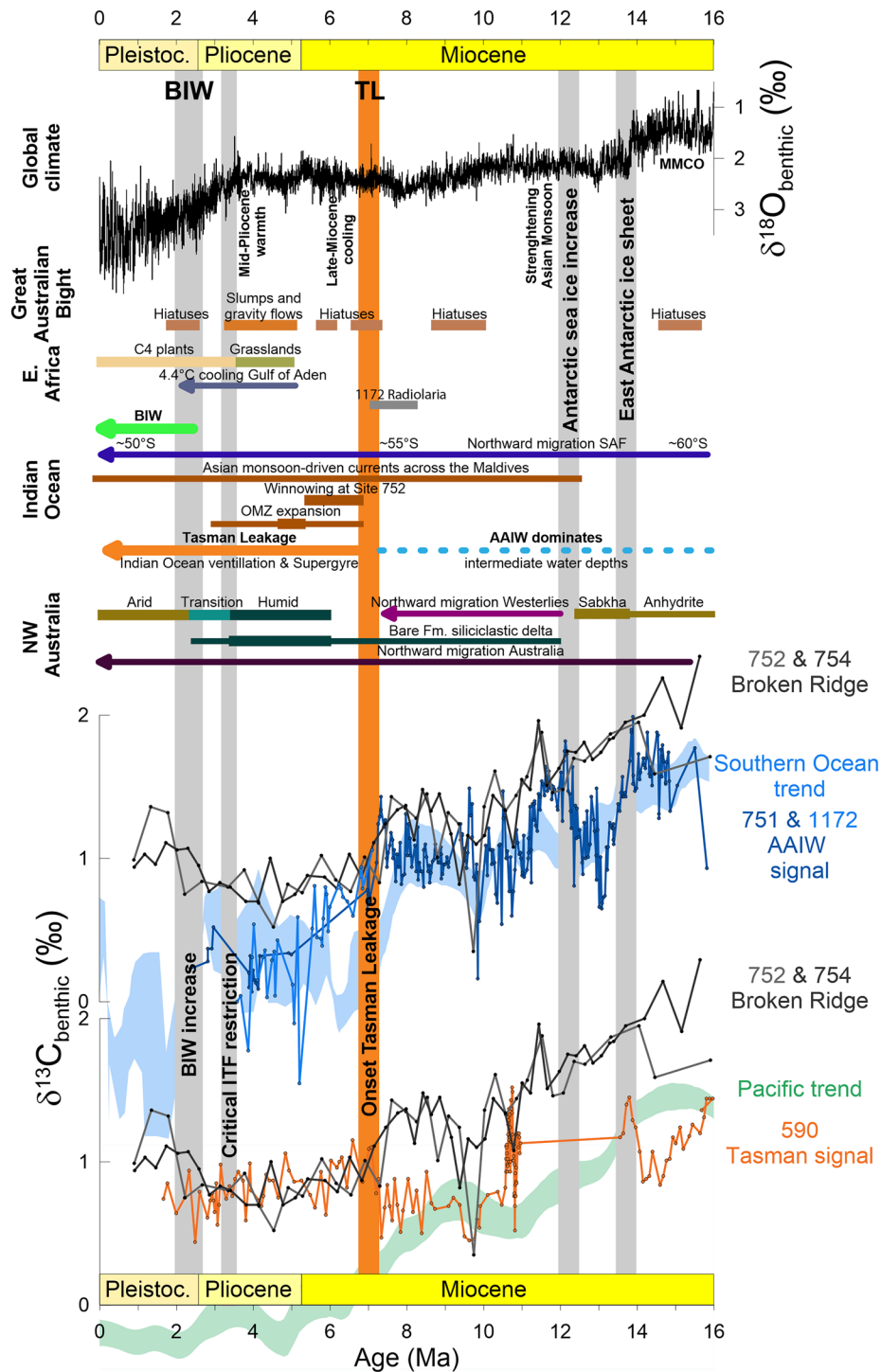
Figure 2. Regional and global events in the context of a ~7 Ma TL onset. The $\delta^{13}C_{benthic}$ signatures of present-day TL end-member Sites (590, 752, and 754) converge at ~7 Ma. At the same time, Broken Ridge Sites 752 and 754 diverge from the AAIW end-member (Sites 751 and 1172). Southern and Pacific Ocean $\delta^{13}C_{benthic}$ trends from Poore et al. (2006) and Cramer et al. (2009), respectively. Western Australia data from Christensen et al. (2017), Tagliaro et al. (2018), and Groeneveld et al. (2017). Oxygen Minimum Zone (OMZ) data from Dickens and Owen (1994). Winnowing data from House et al. (1992). SAF position from Groeneveld et al. (2017). Monsoon intensification from Betzler et al. (2016). Global sedimentary changes data from Eberli et al. (2019). Great Australian Bight data from Li et al. (2004) and International Ocean Discovery Program (ODP) Leg 182 Initial Reports (Feary et al., 2000). NE African and Gulf of Aden data from Liddy et al. (2016). Benthic oxygen isotope megasplice from De Vleeschouwer et al. (2017). Abundant radiolaria at Site 1172 from Diester-Haass et al. (2006) supplement.

4. Discussion: TL and Indian Ocean Circulation

Australia's northward motion led to the progressive uplift of the maritime continent and drove climate change in Australia (Christensen et al., 2017; Groeneveld et al., 2017; Sniderman et al., 2016), and altered surface (Auer et al., 2019; De Vleeschouwer et al., 2018, 2019; Smith et al., 2020) and deeper (Karas et al., 2009, 2011a, 2011b) water circulation. Australia's northward motion progressively constricted the ITF, defining the northern limb of the SHS. Australia's tectonic motion also opened an oceanic gateway to its south, setting up the southern limb of the SHS by creating physical space for westward intermediate water flow north of the ACC.

The late Miocene position of Australia and Tasmania created a southwestern pathway for waters leaving the Tasman Sea to flow around the Tasman Plateau. Critically, at this time, Tasmania sat north of the Subantarctic Front (SAF; Nelson & Cooke, 2010), outside of the main ACC circulation. Southern Australia's migration out of this polar front was mapped using faunal and isotopic values in the Southern Ocean south of New Zealand (Nelson & Cooke, 2010) and is expressed in our study area by a rapid drop in radiolarian abundance at ~7 Ma at ODP Site 1172 (located at 43°S today; Diester-Haass et al., 2006; Figure 2). It is also supported by the Groeneveld et al. (2017) study that documents a concurrent southerly shift in the subantarctic front and westerlies. Once Australia sat north of the SAF, the ACC's oceanographic barrier to westward flow was removed, facilitating TL and SHS onset. While it is possible that waters may have flowed west along this pathway before 7 Ma, aided by shifting westerlies (Groeneveld et al., 2017), modeling suggests the position of the STF here is controlled less by wind belts and more by topography (De Boer et al., 2013). In other words, there is no evidence for sustained TL before 7 Ma. Two intriguing intervals of convergence between the Broken Ridge and TL records at ~10.5 and 9.5 Ma might be evidence for short windows permitted by a southward shift in both westerlies and the STF (Groeneveld et al., 2017). However, these windows likely failed as attempts at TL onset as the more southerly position of Australia would have inhibited extensive flow by Pacific-sourced intermediate waters at those times.

We postulate that the early TL water mass was similar to the modern: waters sourced dominantly from Tasman or Coral Sea thermocline (EAC) waters that persist at upper intermediate depths beyond Tasmania (Figure 1). Unfortunately, there is currently not sufficient data available to test this hypothesis for the Late Miocene. Modern $\delta^{13}C$ values in the region are similar in the Tasman Sea (WOCE Section P06, 2007), GAB (WOCE Section IO9S, 2013), and over the Broken Ridge (WOCE Section IO5E, 2013), ~1‰–1.2‰ (Supporting Information S1). Float data studies by Wong (2005) define three intermediate water pathways in the modern southern Indian Ocean: one east (TL) and one west (AAIW) of the 90E Ridge, and a third along Madagascar mixed with Red Sea waters. We infer the onset of TL at 7 Ma established the precursor to the modern intermediate water pathways, focusing AAIW west of the 90E Ridge and TL to the east, in agreement, again, with the onset of more modern intermediate-deep water circulation at this time (Hodell & Venz-Curtis, 2006).

These inter-site $\delta^{13}C$ patterns suggest that prior to 7 Ma, the intermediate-depth TL pathway was closed for significant inter-basinal transport from the Pacific toward the Indian Ocean. Instead, prior to 7 Ma, the Broken Ridge (Sites 752 and 754) was bathed in oxygen-rich, cold, low-salinity and low-$\delta^{13}C$ intermediate waters sourced from the Southern Ocean (Sites 751 and 1172). This interpretation arises from the similarity between the Broken Ridge records and the deeper water AAIW records (e.g., Site 1088, Billups, 2002; Poore et al., 2006). The fact that the isotopic convergence between the Broken Ridge sites and the Tasman Sea Site 590 is coeval with the isotopic divergence of the Broken Ridge sites from the AAIW sites (Figure 2) advocates a South Pacific gyre connection through the Tasman Sea and the onset of TL at 7 Ma. This interpretation requires the intermediate water pathway south of Australia to be open at 7 Ma. It largely accords with changes in benthic foraminiferal biofacies at ODP Site 757 (90E Ridge) from a well-oxygenated water mass with strong lateral advection to a sustained high flux of organic matter Singh and Gupta (2004) and illustrates the improved connectivity between the Indian and Pacific Oceans (Tasman Leakage).

Sedimentation patterns along the TL pathway (Coral Sea, GAB, and Broken Ridge) also hints at a ~7 Ma TL onset (Figure 2). Gaps in sedimentation in the GAB sites occur at the depth of TL ODP Leg 182 Site 1126, 784 m; Site 1134, 701 m; Site 1130, 488 m (Feary et al., 2004) and act as secondary evidence for enhanced circulation along the TL pathway south of Australia. Grain size data from the Broken Ridge indicates current

winnowing associated with TL onset at 7 Ma (Figure 2; House et al., 1992). In addition, the alignment of Broken Ridge winnowing (House et al., 1992) with evidence for a southerly shift in westerlies (Groeneveld et al., 2017) provides additional support for an atmospheric enhancement to the TL pathway. Interpretation of seismic reflection profiles from ODP Leg 194 Marion Plateau indicates a shift in contourite drift sedimentation at 7.1 Ma (Betzler & Eberli, 2019), supporting enhanced SHS flow in the Coral Sea via the Pacific gyre associated with TL onset. Major changes in the Maldives in the northern Indian Ocean also support an invigorated circulation system ~7 Ma (Figure 2) and a shift toward a more complex Indian Ocean circulation. The Maldives underwent two major changes around the time of the onset of TL: a reduction in upwelling and a change in drift sedimentation by virtue of a N-NE directed bottom current (Betzler et al., 2016), likely driven by enhanced ventilation of the Indian Ocean. These events are coincident with the global peak in biogenic carbonate deposition (or preservation; Diester-Haass et al., 2006; Hermoyian & Owen, 2001).

The global change in depositional character of carbonate banks and platforms supports enhanced global thermohaline circulation (e.g., Hodell & Venz-Curtis, 2006; Keating-Bitonti & Peters, 2019) as predicted by the onset of SHS, and more North Atlantic water reaching the South Atlantic (e.g., Gruetzner et al., 2019). The AAIW ODP sites (751, 757; Figure 2) capture the globally observed LMCIS ~0.8‰ $\delta^{13}C$ shift toward more negative values (e.g., Hodell & Venz-Curtis, 2006; Keigwin, 1979; Keigwin & Shackleton, 1980), which is synchronous in surface and deep waters (Drury et al., 2017, 2018). Tasman Sea Site 590 does not follow the trend of more negative values in the major oceans and instead converges with Sites 752 and 754 by increasing +1‰ as TL turns on, reflecting the influence of EAC-supplied, $\delta^{13}C$–heavier TL waters. The TL records (Sites 590 and 752/754) track one another until the Plio-Pleistocene boundary, when values at the Broken Ridge increase between 2.6 and 1.8 Ma. These dates are associated with the onset of the Arid Interval in NW Australia (Christensen et al., 2017) and enhanced early Pleistocene cooling at Site U1463 (Smith et al., 2020), respectively. The 2.4 Ma onset of the Australian Arid Interval is a manifestation of progressive restriction of the ITF. Concurrence with increasing $\delta^{13}C$ at ODP Sites 752/754 suggests enhanced contributions of ITF–sourced BIW at Broken Ridge as ITF restriction increased inflow of North Pacific waters (Karas et al., 2009). We infer a stronger earliest Pleistocene influence of the northern limb of the SHS at Broken Ridge and greater contributions of more positive $\delta^{13}C$ BIW (Rochford, 1966; Talley & Sprintall, 2005) resulting from continued restriction within the ITF.

Dickens and Owen (1994) interpret a steep decline in Mn and Mn/Sc around 7 Ma at the Broken Ridge as evidence that the Indian Ocean Oxygen Minimum Zone (OMZ) extended that far south. Remarkably, the isotopic divergence between the AAIW and Broken Ridge sites is greatest at ~5 Ma (Figure 2), which corresponds with what (Dickens & Owen, 1994) interpreted as further OMZ intensification at Broken Ridge driven by exceptionally high productivity in the Atlantic, Indian and Pacific Oceans during the latest Miocene and early Pliocene (i.e., the so-called biogenic bloom; Dickens & Owen, 1999). In light of our new understanding of TL onset at this time and its pathway over the Broken Ridge, it is worth exploring the implications. The low-oxygen conditions at Broken Ridge can be explained by [1] *in situ* productivity in the central/southern Indian Ocean during the Biogenic Bloom that led to lower oxygen bottom water conditions at Broken Ridge, [2] the expansion of low-oxygen intermediate waters as far south as Broken Ridge, or by [3] a combination of these two mechanisms. High $CaCO_3$ MAR recorded at the Broken Ridge sites (Peterson et al., 1992) supports high productivity in the surface waters and explanation [1]. Dickens and Owen (1999), on the contrary, argue that the elevated MARs are the result of a reduction in winnowing and ocean circulation (in line with explanation [2]). Benthic foraminiferal analyses at Site 752 indeed evidence low-oxygen availability throughout this interval (Singh et al., 2012), but high variability in these records (Ridha et al., 2019; Singh et al., 2012) suggests that productivity levels were not constant, or that low-oxygen waters were moving in and out of the region. Furthermore, contrary to expectations under model [2], the OMZ event is less intense at the more northerly 90 E Ridge Site 757 (Dickens & Owen, 1999; Singh et al., 2012). We favor explanation [3] and emphasize that the opening of the TL gateway requires a reinterpretation of the benthic foraminiferal ecological variability as a reflection of changing balances between Indian deep waters, the advection of TL waters, and surface water productivity over Broken Ridge.

5. Conclusions

The onset of TL can be discerned in the sedimentary record from 7 Ma onwards. Our study documents Indian Ocean intermediate water dynamics since the middle Miocene and adds an intermediate layer to an increasingly complex view of the global thermohaline circulation. The Broken Ridge records strongly suggest that Indian Ocean intermediate waters were dominated by AAIW until 7 Ma. Afterward, TL initiates and invigorates Indian Ocean circulation. The onset required the Australian continent to move northward, creating space for TL to flow between Australia and the STF. A southerly shift in westerlies and concordant migration of the STF around 7 Ma probably determined the exact timing of TL onset. Thus, the southern hemisphere significantly influenced the re-organization of late Miocene global ocean circulation, complementary to the changes driven by enhanced contribution from the North Atlantic and depicted by the LM-CIS (Gruetzner et al., 2019; Hodell & Venz-Curtis, 2006; Keating-Bitonti & Peters, 2019). In the late Pliocene, Indian Ocean intermediate water dynamics change again when the BIW mainly provide waters from the Northern Pacific, rather than from the equatorial and Southern Pacific, in response to ITF constriction.

The late Miocene onset of the SHS is coeval with many important climatic and oceanographic events, including the LMCIS, establishment of "modern" intermediate waters (Hodell & Venz-Curtis, 2006) and simultaneous peaks in carbonate production between the eastern Pacific and the South Atlantic (Drury et al., 2021). Our study demonstrates that TL turned on at 7 Ma, and therewith provides a new piece of the cause-and-effect chain shaping the major transformation of oceans and climate at that time. However, detailed answers await better high-resolution paleoceanographic records, which in turn await better sediment core and future Ocean drilling. Indeed, numerous questions remain unanswered with the current paleoceanographic data sets. For example, how did the TL onset impact global heat flow? Did it play a direct role in the global cooling at 7 Ma (Herbert et al., 2016), or was its chief contribution that it served as a sentinel for the opening of the TL gateway and the associated oceanic circulation changes? Was this the start of enhanced global thermohaline circulation? Carbonate platform drowning at ~7 Ma on the Marion Plateau (Eberli et al., 2010; Figure 2) further implicates TL and the SHS, suggesting enhanced circulation evident in the Indian Ocean is linked to invigorated global circulation. What controls the variability of surface water productivity and TL at the Broken Ridge in the late Miocene, and did a shift in westerlies aid in the onset of TL? Might this shift in westerlies be the atmospheric link that aids in regional (e.g., Feakins et al., 2020; Tauxe & Feakins, 2020) and global patterns in cooling and drying at 7 Ma? These questions cannot be answered with the available sediments and research cannot progress without high quality core material that will allow for detailed analyses across these critical intervals at locations that define the limits of a heretofore unrecognized limb of global circulation in the sedimentary record. Re-drilling the Broken Ridge to provide suitable material to generate high-resolution proxy records is critical to answering these questions. Likewise, obtaining Miocene–age paleoceanographic records in the Tasman Sea is also paramount to defining the role of TL and the SHS in global circulation.

Data Availability Statement

The data on which this article are based are available in Kennett (1986), Mackensen et al. (1992), Rea et al. (1991); House et al. (1992), and Diester-Haas et al., (2006). Original data were accessed from the Pangaea and NOAA geoscientific data repositories (Site 590: https://doi.org/10.1594/PANGAEA.729770, Site 751: https://doi.org/10.1594/PANGAEA.760328, Sites 752, 754, and 757: https://doi.org/10.1594/PANGAEA.758956, https://doi.org/10.1594/PANGAEA.759769, and Site 1172A: https://doi.org/10.1594/PANGAEA.835082). Updated age models are found at Zenodo.org (https://doi.org/10.5281/zenodo.5341054).

References

Auer, G., De Vleeschouwer, D., Smith, R. A., Bogus, K., Groeneveld, J., Grunert, P., et al. (2019). Timing and Pacing of Indonesian Throughflow Restriction and Its Connection to Late Pliocene Climate Shifts. *Paleoceanography and Paleoclimatology*, *34*(4), 635–657. https://doi.org/10.1029/2018pa003512

Behrens, E., Fernandez, D., & Sutton, P. (2019). Meridional oceanic heat transport influences marine heatwaves in the Tasman Sea on interannual to decadal timescales. *Frontiers in Marine Science*, *6*. https://doi.org/10.3389/fmars.2019.00228

Betzler, C., & Eberli, G. P. (2019). Miocene start of modern carbonate platforms. *Geology*, *47*(8), 771–775. https://doi.org/10.1130/g45994.1

Betzler, C., Eberli, G. P., Kroon, D., Wright, J. D., Swart, P. K., Nath, B. N., et al. (2016). The abrupt onset of the modern South Asian Monsoon winds. *Scientific Reports*, *6*, 29838. https://doi.org/10.1038/srep29838. Retrieved from https://www.ncbi.nlm.nih.gov/pubmed/27436574

Billups, K. (2002). Late Miocene through early Pliocene deep water circulation and climate change viewed from the sub-Antarctic South Atlantic. *Palaeogeography, Palaeoclimatology, Palaeoecology*, *185*, 287–307. https://doi.org/10.1016/s0031-0182(02)00340-1

Christensen, B. A., Renema, W., Henderiks, J., De Vleeschouwer, D., Groeneveld, J., Castañeda, I. S., et al. (2017). Indonesian through flow drove Australian climate from humid Pliocene to arid Pleistocene. *Geophysical Research Letters*, *44*(13), 6914–6925. https://doi.org/10.1002/2017GL072977

Cramer, B. S., Toggweiler, J. R., Wright, J. D., Katz, M. E., & Miller, K. G. (2009). Ocean overturning since the Late Cretaceous: Inferences from a new benthic foraminiferal isotope compilation. *Paleoceanography*, *24*(4). https://doi.org/10.1029/2008PA001683

De Boer, A. M., Graham, R. M., Thomas, M. D., & Kohfeld, K. E. (2013). The control of the Southern Hemisphere Westerlies on the position of the subtropical front. *Journal of Geophysical Research: Oceans*, *118*(10), 5669–5675. https://doi.org/10.1002/jgrc.20407

De Vleeschouwer, D., Auer, G., Smith, R., Bogus, K., Christensen, B., Groeneveld, J., et al. (2018). The amplifying effect of Indonesian Through flow heat transport on Late Pliocene Southern Hemisphere climate cooling. *Earth and Planetary Science Letters*, *500*, 15–27. https://doi.org/10.1016/j.epsl.2018.07.035. Retrieved from http://www.sciencedirect.com/science/article/pii/S0012821X18304412

De Vleeschouwer, D., Petrick, B. F., & Martínez-García, A. (2019). Stepwise Weakening of the Pliocene Leeuwin Current. *Geophysical Research Letters*, *46*(14), 8310–8319. https://doi.org/10.1029/2019gl083670

De Vleeschouwer, D., Vahlenkamp, M., Crucifix, M., & Pälike, H. (2017). Alternating Southern and Northern Hemisphere climate response to astronomical forcing during the past 35 m. *Geology*, *45*(4), 375–378. https://doi.org/10.1130/g38663.1

Dickens, G. R., & Owen, R. M. (1994). Late Miocene-Early Pliocene manganese redirection in the central Indian Ocean: Expansion of the intermediate water oxygen minimum zone. *Paleoceanography*, *9*(1), 169–181. https://doi.org/10.1029/93PA02699

Dickens, G. R., & Owen, R. M. (1999). The Latest Miocene–Early Pliocene biogenic bloom: A revised Indian Ocean perspective. *Marine Geology*, *161*(1), 75–91. https://doi.org/10.1016/s0025-3227(99)00057-2

Diester-Haass, L., Billups, K., & Emeis, K. C. (2006). Late Miocene carbon isotope records and marine biological productivity: Was there a (dusty) link? *Paleoceanography*, *21*(4). https://doi.org/10.1029/2006PA001267

Drury, A. J., Lee, G. P., Gray, W. R., Lyle, M., Westerhold, T., Shevenell, A. E., & John, C. M. (2018). Deciphering the State of the Late Miocene to Early Pliocene Equatorial Pacific. *Paleoceanography and Paleoclimatology*, *33*(3), 246–263. https://doi.org/10.1002/2017pa003245

Drury, A. J., Liebrand, D., Westerhold, T., Beddow, H. M., Hodell, D. A., Rohlfs, N., et al. (2021). Climate, cryosphere and carbon cycle controls on Southeast Atlantic orbital-scale carbonate deposition since the Oligocene (30–0 Ma). *Climate of the Past*. https://doi.org/10.5194/cp-2020-108

Drury, A. J., Westerhold, T., Frederichs, T., Tian, J., Wilkens, R., Channell, J. E. T., et al. (2017). Late Miocene climate and time scale reconciliation: Accurate orbital calibration from a deep-sea perspective. *Earth and Planetary Science Letters*, *475*, 254–266. https://doi.org/10.1016/j.epsl.2017.07.038. Retrieved from http://www.sciencedirect.com/science/article/pii/S0012821X17304223

Duan, Y., Hou, Y., Liu, H., & Liu, Y. (2013). The water mass variability and southward shift of the Southern Hemisphere mid-depth super-gyre. *Acta Oceanologica Sinica*, *32*(11), 74–81. https://doi.org/10.1007/s13131-013-0380-7

Durgadoo, J. V., Rühs, S., Biastoch, A., & Böning, C. W. B. (2017). Indian Ocean sources of Agulhas leakage. *Journal of Geophysical Research: Oceans*, *122*(4), 3481–3499. https://doi.org/10.1002/2016jc012676

Eberli, G. P., Anselmetti, F. S., Isern, A. R., & Delius, H. (2010). Timing of changes in sea-level and currents along miocene platforms on the Marion plateau. In *Cenozoic Carbonates of Central Australasia*. SEPM (Society for Sedimentary Geology).

Eberli, G. P., Betzler, C., & Frank, T. (2019). Characteristics of modern carbonate contourite drifts. *Sedimentology*, *66*(4), 1163–1191. https://doi.org/10.1111/sed.12584

Fan, L., Guan, H., Cai, W., Rofe, C. P., & Xu, J. (2020). A 7-year lag precipitation teleconnection in South Australia and its possible mechanism. *Frontiers in Earth Science*, *8*. https://doi.org/10.3389/feart.2020.553506

Feakins, S. J., Liddy, H. M., Tauxe, L., Galy, V., Feng, X., Tierney, J. E., et al. (2020). Miocene C4 Grassland expansion as recorded by the Indus fan. *Paleoceanography and Paleoclimatology*, *35*(7), 18. https://doi.org/10.1029/2020pa003856

Feary, D. A., Hine, A. C., James, N. P., & Malone, M. J. (2004). LEg 182 Synthesis: Exposed Secrets of the Great Australian Bight. In *Proceedings of the Ocean Drilling Program* (Vol. 182). Scientific Results. https://doi.org/10.2973/odp.proc.sr.182.017.2004

Feary, D. A., Hine, A. C., Malone, M. J., (Eds). (2000). *Proceedings of the Ocean Drilling Program, 182 Initial Reports*. Ocean Drilling Program. https://doi.org/10.2973/odp.proc.ir.182.2000

Gradstein, F. M., Ogg, J. G., & Hilgen, F. J. (2012). On the geologic time scale. *Newsletters on Stratigraphy*, *45*(2), 171–188. https://doi.org/10.1127/0078-0421/2012/0020

Groeneveld, J., Henderiks, J., Renema, W., McHugh, C. M., De Vleeschouwer, D., Christensen, B. A., et al. (2017). Australian shelf sediments reveal shifts in Miocene Southern Hemisphere westerlies. *Science Advances*, *3*, 8. https://doi.org/10.1126/sciadv.1602567

Gruetzner, J., Jiménez Espejo, F. J., Lathika, N., Uenzelmann-Neben, G., Hall, I. R., Hemming, S. R., & LeVay, L. J. (2019). A new seismic stratigraphy in the Indian-Atlantic Ocean gateway resembles major Paleo-Oceanographic changes of the last 7 Ma. *Geochemistry, Geophysics, Geosystems*, *20*(1), 339–358. https://doi.org/10.1029/2018gc007668

Herbert, T. D., Lawrence, K. T., Tzanova, A., Peterson, L. C., Caballero-Gill, R., & Kelly, C. S. (2016). Late Miocene global cooling and the rise of modern ecosystems. *Nature Geoscience*, *9*(11), 843–847. https://doi.org/10.1038/ngeo2813

Hermoyian, C. S., & Owen, R. M. (2001). Late Miocene-early Pliocene biogenic bloom: Evidence from low-productivity regions of the Indian and Atlantic Oceans. *Paleoceanography*, *16*(1), 95–100. https://doi.org/10.1029/2000pa000501

Hodell, D. A., & Venz-Curtis, K. A. (2006). Late Neogene history of deepwater ventilation in the Southern Ocean. *Geochemistry, Geophysics, Geosystems*, *7*(9). https://doi.org/10.1029/2005gc001211

House, M., Rea, D. K., & Janecek, T. R. (1992). Grain-size record of ocean current winnowing in Oligocene to Pleistocene ooze, Broken Ridge, Southeastern Indian Ocean. *Proceedings of the Ocean Drilling Program, Scientific Results*, *121*, 211–218.

Hu, D., Wu, L., Cai, W., Gupta, A. S., Ganachaud, A., Qiu, B., et al. (2015). Pacific western boundary currents and their roles in climate. *Nature*, *522*(7556), 299–308. https://doi.org/10.1038/nature14504. Retrieved from https://www.ncbi.nlm.nih.gov/pubmed/26085269

Huck, C. E., van de Flierdt, T., Bohaty, S. M., & Hammond, S. J. (2017). Antarctic climate, Southern Ocean circulation patterns, and deep water formation during the Eocene. *Paleoceanography*, *32*(7), 674–691. https://doi.org/10.1002/2017pa003135

Isern, A. R., Anselmetti, F. S., & Blum, P. (2002). Leg 194 summary. *Proceedings of the Ocean Drilling Program*, *194*, 1–88. https://doi.org/10.2973/odp.proc.ir.194.101.2002

Karas, C., Nürnberg, D., Gupta, A. K., Tiedemann, R., Mohan, K., & Bickert, T. (2009). Mid-Pliocene climate change amplified by a switch in Indonesian subsurface Throughflow. *Nature Geoscience*, *2*(6), 434–438. https://doi.org/10.1038/ngeo520

Karas, C., Nürnberg, D., Tiedemann, R., & Garbe-Schönberg, D. (2011a). Pliocene climate change of the Southwest Pacific and the impact of ocean gateways. *Earth and Planetary Science Letters*, *301*(1–2), 117–124. https://doi.org/10.1016/j.epsl.2010.10.028

Karas, C., Nürnberg, D., Tiedemann, R., & Garbe-Schönberg, D. (2011b). Pliocene Indonesian Throughflow and Leeuwin Current dynamics: Implications for Indian Ocean polar heat flux. *Paleoceanography*, *26*(2). https://doi.org/10.1029/2010pa001949

Keating-Bitonti, C. R., & Peters, S. E. (2019). Influence of increasing carbonate saturation in Atlantic bottom water during the late Miocene. *Palaeogeography, Palaeoclimatology, Palaeoecology*, *518*, 134–142. https://doi.org/10.1016/j.palaeo.2019.01.006

Keigwin, L. D., Jr. (1979). Late Cenozoic stable isotope stratigraphy and paleoceanography of DSDP Sites from the East Equatorial and Central North Pacific Ocean. *Earth and Planetary Science Letters*, *45*, 21. https://doi.org/10.1016/0012-821x(79)90137-7

Keigwin, L. D., & Shackleton, N. J. (1980). Uppermost Miocene carbon isotope stratigraphy of a piston core in the equatorial Pacific. *Nature*, *284*(17), 613–614. https://doi.org/10.1038/284613a0

Kennett, J. P. (1986). Miocene to early Pliocene oxygen and carbon isotope stratigraphy in the southwest Pacific, Deep Sea Drilling Project Leg 90. Initial reports of the Deep Sea Drilling Project. *Legal Times*, *90*, 29. https://doi.org/10.2973/dsdp.proc.90.142.1986

Li, Q., Simo, J. A., McGowran, B., & Holbourn, A. (2004). The eustatic and tectonic origin of Neogene unconformities from the Great Australian Bight. *Marine Geology*, *203*(1–2), 57–81. https://doi.org/10.1016/s0025-3227(03)00329-3

Liddy, H. M., Feakins, S. J., & Tierney, J. E. (2016). Cooling and drying in northeast Africa across the Pliocene. *Earth and Planetary Science Letters*, *449*, 430–438. https://doi.org/10.1016/j.epsl.2016.05.005

Lumpkin, R., & Speer, K. (2007). Global Ocean meridional overturning. *Journal of Physical Oceanography*, *37*(10), 2550–2562. https://doi.org/10.1175/jpo3130.1

Mackensen, A., Barrera, E., & Hubberten, H.-W. (1992). Neogene circulation in the southern Indian Ocean: Evidence from benthic foraminifers, carbonate data, and stable isotope analyses (Site 751). *Proceedings of the Ocean Drilling Program, Scientific Results*, *120*, 867–878. https://doi.org/10.2973/odp.proc.sr.120.169.1992

Nelson, C. S., & Cooke, P. J. (2010). History of oceanic front development in the New Zealand sector of the Southern Ocean during the Cenozoic—A synthesis. *New Zealand Journal of Geology and Geophysics*, *44*(4), 535–553. https://doi.org/10.1080/00288306.2001.9514954

Oliver, E. C. J., O'Kane, T. J., & Holbrook, N. J. (2015). Projected changes to Tasman Sea eddies in a future climate. *Journal of Geophysical Research: Oceans*, *120*(11), 7150–7165. https://doi.org/10.1002/2015jc010993

Peterson, L. C., Murray, D. W., Ehrmann, W. U., & Hempel, P. (1992). *Cenozoic carbonate accumulation and compensation depth changes in the Indian Ocean*.

Poore, H. R., Samworth, R., White, N. J., Jones, S. M., & McCave, I. N. (2006). Neogene overflow of Northern component water at the Greenland-Scotland Ridge. *Geochemistry, Geophysics, Geosystems*, *7*(6). https://doi.org/10.1029/2005gc001085

Qu, T., Fukumori, I., & Fine, R. A. (2019). Spin-Up of the Southern Hemisphere Super Gyre. *Journal of Geophysical Research: Oceans*, *124*(1), 154–170. https://doi.org/10.1029/2018jc014391

Rea, D. K., Lohmann, K. C., MacLeod, N. D., House, M. A., Hovan, S. A., & Martin, G. D. (1991). Oxygen and carbon isotopic records from the oozes of Sites 752,754,756, AND 757, Eastern Indian Ocean. *Proceedings of the Ocean Drilling Program, Scientific Results*, *121*. https://doi.org/10.2973/odp.proc.sr.121.130.1991

Ridgway, K. R., & Dunn, J. R. (2003). Mesoscale structure of the mean East Australian Current System and its relationship with topography. *Progress in Oceanography*, *56*(2), 189–222. https://doi.org/10.1016/s0079-6611(03)00004-1

Ridgway, K. R., & Dunn, J. R. (2007). Observational evidence for a Southern Hemisphere oceanic supergyre. *Geophysical Research Letters*, *34*(13). https://doi.org/10.1029/2007gl030392

Ridha, D., Boomer, I., & Edgar, K. M. (2019). Latest Oligocene to earliest Pliocene deep-sea benthic foraminifera from Ocean Drilling Program (ODP) Sites 752, 1168 and 1139, southern Indian Ocean. *Journal of Micropalaeontology*, *38*(2), 189–229. https://doi.org/10.5194/jm-38-189-2019

Rintoul, S. R., & Bullister, J. L. (1999). A late winter hydrographic section from Tasmania to Antarctica. *Deep-Sea Research I*, *46*, 1417–1454. https://doi.org/10.1016/s0967-0637(99)00013-8

Rintoul, S. R., & Sokolov, S. (2001). Baroclinic transport variability of the Antarctic Circumpolar Current south of Australia (WOCE repeat section SR3). *Journal of Geophysical Research*, *106*(C2), 2815–2832. https://doi.org/10.1029/2000jc900107

Rochford, D. J. (1966). Distribution of Banda intermediate water in the Indian Ocean. *Australian Journal of Marine & Freshwater Research*, *17*, 61–76. https://doi.org/10.1071/mf9660061

Rosell-Fieschi, M., Rintoul, S. R., Gourrion, J., & Pelegrí, J. L. (2013). Tasman Leakage of intermediate waters as inferred from Argo floats. *Geophysical Research Letters*, *40*(20), 5456–5460. https://doi.org/10.1002/2013gl057797

Rousselet, L., Cessi, P., & Forget, G. (2020). Routes of the upper branch of the Atlantic Meridional overturning circulation according to an Ocean state estimate. *Geophysical Research Letters*, *47*(18), e2020GL089137. https://doi.org/10.1029/2020gl089137. Retrieved from https://www.ncbi.nlm.nih.gov/pubmed/33380755

Schott, F. A., Xie, S.-P., & McCreary, J. P. (2009). Indian Ocean circulation and climate variability. *Reviews of Geophysics*, *47*(1). https://doi.org/10.1029/2007rg000245

Singh, R. K., & Gupta, A. K. (2004). Late Oligocene–Miocene paleoceanographic evolution of the southeastern Indian Ocean: Evidence from deep-sea benthic foraminifera (ODP Site 757). *Marine Micropaleontology*, *51*(1), 153–170. https://doi.org/10.1016/j.marmicro.2003.10.003

Singh, R. K., Gupta, A. K., & Das, M. (2012). Paleoceanographic significance of deep-sea benthic foraminiferal species diversity at southeastern Indian Ocean Hole 752A during the Neogene. *Palaeogeography, Palaeoclimatology, Palaeoecology*, *361–362*, 94–103. https://doi.org/10.1016/j.palaeo.2012.08.008

Sloyan, B. M., & Rintoul, S. R. (2001). Circulation, renewal, and modification of Antarctic mode and intermediate water. *Journal of Physical Oceanography*, *31*, 25. https://doi.org/10.1175/1520-0485(2001)031<1005:cramoa>2.0.co;2

Smith, R. A., Castañeda, I. S., Groeneveld, J., De Vleeschouwer, D., Henderiks, J., Christensen, B. A., et al. (2020). Plio-Pleistocene Indonesian Throughflow variability drove Eastern Indian Ocean sea surface temperatures. *Paleoceanography and Paleoclimatology*, *35*(10). https://doi.org/10.1029/2020pa003872

Sniderman, J. M., Woodhead, J. D., Hellstrom, J., Jordan, G. J., Drysdale, R. N., Tyler, J. J., & Porch, N. (2016). Pliocene reversal of late Neogene aridification. *Proceedings of the National Academy of Sciences of the United States of America*, *113*(8), 1999–2004. https://doi.org/10.1073/pnas.1520188113. Retrieved from https://www.ncbi.nlm.nih.gov/pubmed/26858429

Speich, S., Blanke, B., & Cai, W. (2007). Atlantic meridional overturning circulation and the Southern Hemisphere supergyre. *Geophysical Research Letters*, *34*(23). https://doi.org/10.1029/2007gl031583

Speich, S., Blanke, B., de Vries, P., Drijfhout, S., Döös, K., Ganachaud, A., & Marsh, R. (2002). Tasman leakage: A new route in the global ocean conveyor belt. *Geophysical Research Letters*, *29*(10). https://doi.org/10.1029/2001gl014586

Tagliaro, G., Fulthorpe, C. S., Gallagher, S. J., McHugh, C. M., Kominz, M., & Lavier, L. L. (2018). Neogene siliciclastic deposition and climate variability on a carbonate margin: Australian Northwest Shelf. *Marine Geology*, *403*, 285–300. https://doi.org/10.1016/j.margeo.2018.06.007

Talley, L. (2013). Closure of the global overturning circulation Through the Indian, Pacific, and Southern Oceans: Schematics and transports. *Oceanography*, *26*(1), 80–97. https://doi.org/10.5670/oceanog.2013.07

Talley, L. D. (2013). *Hydrographic atlas of the world ocean circulation experiment (WOCE)* (Vol. 4). Indian OceanInternational WOCE Project Office.

Talley, L. D., & Sprintall, J. (2005). Deep expression of the Indonesian Throughflow: Indonesian Intermediate Water in the South Equatorial Current. *Journal of Geophysical Research*, *110*(C10). https://doi.org/10.1029/2004jc002826

Tauxe, L., & Feakins, S. J. (2020). A Reassessment of the chronostratigraphy of Late Miocene C3–C4 transitions. *Paleoceanography and Paleoclimatology*, *35*(7). https://doi.org/10.1029/2020pa003857

Tian, J., Ma, X., Zhou, J., Jiang, X., Lyle, M., Shackford, J., & Wilkens, R. (2018). Paleoceanography of the east equatorial Pacific over the past 16 Myr and Pacific–Atlantic comparison: High resolution benthic foraminiferal δ18O and δ13C records at IODP Site U1337. *Earth and Planetary Science Letters*, *499*, 185–196. https://doi.org/10.1016/j.epsl.2018.07.025

Tilburg, C. E., Hurlburt, H. E., O'Brien, J. J., & Shriver, J. F. (2001). The dynamics of the East Australian Current System: The Tasman Front, the East Auckland Current, and the East Cape Current. *Journal of Physical Oceanography*, *31*, 26. https://doi.org/10.1175/1520-0485(2001)031<2917:tdotea>2.0.co;2

van Sebille, E., England, M. H., Zika, J. D., & Sloyan, B. M. (2012). Tasman leakage in a fine-resolution ocean model. *Geophysical Research Letters*, *39*(6). https://doi.org/10.1029/2012gl051004

van Sebille, E., Sprintall, J., Schwarzkopf, F. U., Sen Gupta, A., Santoso, A., England, M. H., et al. (2014). Pacific-to-Indian Ocean connectivity: Tasman leakage, Indonesian Throughflow, and the role of ENSO. *Journal of Geophysical Research: Oceans*, *119*(2), 1365–1382. https://doi.org/10.1002/2013jc009525

Wong, A. P. S. (2005). Sub Antarctic mode water and Antarctic Intermediate Water in the South Indian Ocean based on profiling float data 2000–2004. *Journal of Marine Research*, *63*(4), 789–812. https://doi.org/10.1357/0022240054663196

References From the Supporting Information

Bagley, J. C., & Johnson, J. B. (2014). Phylogeography and biogeography of the lower Central American Neotropics: Diversification between two continents and between two seas. *Biological Reviews of the Cambridge Philosophical Society*, *89*(4), 767–790. https://doi.org/10.1111/brv.12076. Retrieved from https://www.ncbi.nlm.nih.gov/pubmed/24495219

Bull, C. Y. S., Kiss, A. E., Jourdain, N. C., England, M. H., & van Sebille, E. (2017). Wind forced variability in Eddy Formation, Eddy Shedding, and the separation of the East Australian Current. *Journal of Geophysical Research: Oceans*, *122*(12), 9980–9998. https://doi.org/10.1002/2017jc013311

Duran, E. R., Phillips, H. E., Furue, R., Spence, P., & Bindoff, N. L. (2020). Southern Australia Current System based on a gridded hydrography and a high-resolution model. *Progress in Oceanography*, *181*. https://doi.org/10.1016/j.pocean.2019.102254

Feng, M., Zhang, X., Oke, P., Monselesan, D., Chamberlain, M., Matear, R., & Schiller, A. (2016). Invigorating ocean boundary current systems around Australia during 1979–2014: As simulated in a near-global eddy-resolving ocean model. *ournal of Geophysical Research: Oceans*, *121*(5), 3395–3408. https://doi.org/10.1002/2016JC011842

Graham, R. M., & De Boer, A. M. (2013). The dynamical subtropical front. *Journal of Geophysical Research: Oceans*, *118*(10), 5676–5685. https://doi.org/10.1002/jgrc.20408

Hall, R. (2009). Southeast Asia's changing palaeogeography. *Blumea–Biodiversity, Evolution and Biogeography of Plants*, *54*(1), 148–161. https://doi.org/10.3767/000651909x475941

Middleton, J. F., & Cirano, M. (2005). Wintertime circulation off southeast Australia: Strong forcing by the East Australian Current. *Journal of Geophysical Research*, *110*(C12). https://doi.org/10.1029/2004jc002855

Park, Y. H., Park, T., Kim, T. W., Lee, S. H., Hong, C. S., Lee, J. H., et al. (2019). Observations of the Antarctic Circumpolar Current over the Udintsev fracture zone, the narrowest choke point in the Southern Ocean. *Journal of Geophysical Research: Oceans*, *124*(7), 4511–4528. https://doi.org/10.1029/2019jc015024

Rögl, F. (1999). Mediterranean and Paratethys. Facts and hypotheses of an Oligocene to Miocene paleogeography (short overview). *Geologica Carpathica*, *50*, 339–349.

Suthers, I. M., Young, J. W., Baird, M. E., Roughan, M., Everett, J. D., Brassington, G. B., et al. (2011). The strengthening East Australian Current, its Eddies and biological effects—an introduction and overview. *Deep Sea Research Part II: Topical Studies in Oceanography*, *58*(5), 538–546. https://doi.org/10.1016/j.dsr2.2010.09.029

Sutton, P. J. H., & Bowen, M. (2014). Flows in the Tasman Front south of Norfolk Island. *Journal of Geophysical Research: Oceans*, *119*(5), 3041–3053. https://doi.org/10.1002/2013jc009543

Talley, L. D. (2007). Hydrographic atlas of the World Ocean circulation experiment (WOCE). In *Pacific Ocean* (Vol. 2). International WOCE Project Office.

Talley, Y. (1998). Dianeutral mixing and transformation of Antarctic Intermediate Water in the Indian Ocean. *Journal of Geophysical Research*, *103*(C13), 30941–30971. https://doi.org/10.1029/1998jc900008

Ypma, S. L., van Sebille, E., Kiss, A. E., & Spence, P. (2016). The separation of the East Australian Current: A Lagrangian approach to potential vorticity and upstream control. *Journal of Geophysical Research: Oceans*, *121*(1), 758–774. https://doi.org/10.1002/2015jc011133